Petroleum & Coal
ISSN 1337-7027

Available online at www.vurup.sk/petroleum-coal
Petroleum & Coal 56 (1) 41-53, 2014

APPLICATION OF ROCK AND SEISMIC PROPERTIES FOR PREDICTION OF HYDROCARBON POTENTIAL

*Oluwatosin J. Rotimi[1,2], Bankole D. Ako[3], Wang Zhenli[2]

[1]Petroleum Engineering Department, Covenant University, Ota, Nigeria;[2]Key Laboratory of Petroleum Resources, Institute of Geology and Geophysics, CAS, Beijing, China
[3]Department of Applied Geophysics, Federal University of Technology, Akure, Nigeria
*Email – oluwatosin.rotimi@covenantuniversity.edu.ng, tossynrotimmy@yahoo.com

Received September 26, 2013, Accepted January 15, 2014

Abstract

This study explores the use of well logs and seismic derived rock properties to predict hydrocarbon potentials. Crossplot analysis of well log data and seismic attributes extracted and captured over some depth windows from the vicinity of the prolific hydrocarbon zone was the main methodology. This made it possible to develop relationships through cross-plotting of different log types and different seismic attributes. Emphasis was placed on petrophysics based properties from well logs while the stratigraphic, complex and signal based seismic attributes were computed and analysed. Combination of one or more attributes was attempted in deriving a correlative relationship typifying the reservoir property.
The well log derived properties predicted the hydrocarbon potential of the reservoir better as it gave better correlation of above 70% on the crossplots made. While seismic properties crossplots had poor correlation except those of signal based and complex attributes that gave negative correlations.

Keywords: well logs; seismic; hydrocarbon; attributes; petrophysics; reservoir; extracted.

1. Introduction

Harnessing the full potential of reservoir rocks from exploration data such as well logs and seismic data is the goal of explorationists. Extracting petrophysical properties or other rock properties from reservoir column of the subsurface needs a closer observation and evaluation of the data derived for this region of interest. Well logs refer to records taken of various properties of subsurface formations encountered during drilling operations. In practice, the most useful of the geophysical logging methods are those that are used to unravel lithology, saturation, porosity and petrophysical properties of the formations [1].

Seismic data is derived from measurement of responses of pulse of waves sent to the subsurface from a source point and received by an acoustic receiver that takes measurement in response to ground vibration or anomalous hydraulic pressures in the water body for marine survey [2]. The total energy of the transmitted and reflected ray equals the energy of the incident ray. The relative proportions of energy transmitted and reflected are determined by the contrast in Acoustic impedance (**Z**) across the interface while elasticity deals with deformation that vanishes completely upon removal of the stress which caused the deformation, such as from the passage of a seismic wave [3].

M. T. Taner *et al.* [4] classified attributes into two general categories: geometrical and physical. The objective of geometrical attributes is to enhance the visibility of the geometrical characteristics of seismic data; they include dip, azimuth, and continuity. Physical attributes have to do with the physical parameters of the subsurface and so relate to lithology. These include amplitude, phase, and frequency. [5-7] classified attributes using a tree structure with time, amplitude, frequency, and attenuation as the main branches, which further branch out into poststack and prestack categories. Time attributes provide information on structure, whereas amplitude attributes provide information on stratigraphy and reservoir.

When using attributes for the quantitative prediction of rock properties, it is important to remember the relations and equations presented in [8-11] because they formulate the physical relationship between the seismic attribute and rock and fluid properties.

Amplitude, phase, and frequency are fundamental parameters of the seismic wavelet and from these few, all other attributes are derived, either singly or in combinations, and many of the new attributes duplicate each other because of the nature of the computations. For example, bi-variate scatter plots of amplitude variance, average energy, RMS amplitude, reflection strength, and average absolute amplitude show either a linear or parabolic relationship [12-13].

The proliferation of new attributes necessitated a combination of attributes that may not make sense individually. For example, a high negative correlation between porosity and acoustic impedance has a physical basis, because velocity has an inverse relationship to porosity; as velocity increases, the porosity typically decreases. Selection of attributes may be based on the strength of observed correlations with properties measured at the wells. The objective of this study is to establish the property that best predicts and characterize hydrocarbon saturation for the clastic reservoir of this area.

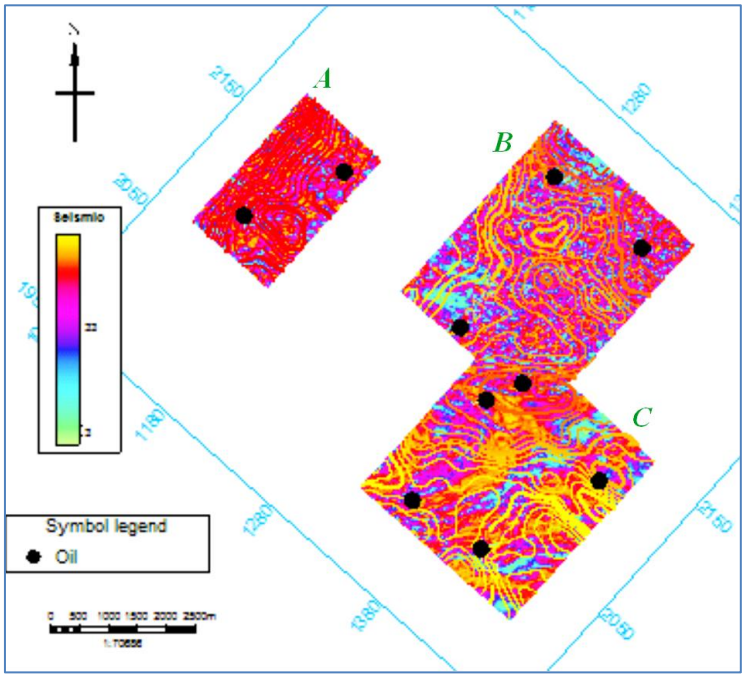

Figure 1 Seismic RMS amplitude property surface maps of the three regions of interest studied

2. Methodology

In defining relationships between petrophysical properties and seismic properties it was important to concentrate effort on locations within the field of study that is proven to have high hydrocarbon saturation and also focus on vicinity with well data as control point for property values distribution in the modeled zone. An attempt was made to decompartmentalize the zone interpreted into smaller regions of interest (Figure 1), from where in a closer view of the rock properties can be taken. To achieve this, the survey acquisition bin size, the structural orientation and prevalent stratigraphic pattern is used with the powerful horizon probe utility of the Petrel software to carve out three distinctive horizon-zone volume probe from which the relationship deductions were made (Figures 1 - 3). For the three horizon cube region of interest (ROI), specific properties were sampled into the spatially informative seismic resolution from the various depth converted properties earlier modeled in a simulation case for property modeling. In addition to the reservoir rock properties sampled into seismic resolution, seismic attributes of interests were also computed from the raw seismic and also from the post-stack inversion. Some extra computations done stemmed from complex, structural and stratigraphic attributes computed from the raw amplitude seismic. To guide against error and disparity in scale, the depth converted seismic data was used a full stop. Layering of the simulation case built was made as fine as necessary accounting for details

which is a function of the thinnest interpretable formation on the well log data. With the prior knowledge of the resolution of well logging operation the choice of layer thickness was made and accounts well for different portion of the zone in its varied thickness.

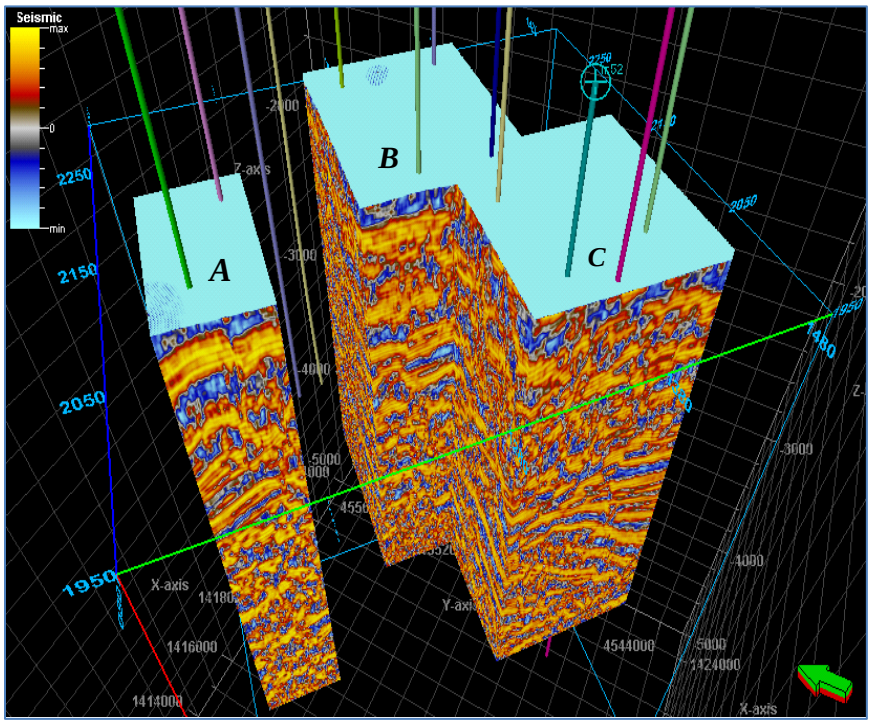

Figure 2 Regions of interest (ROI) RMS amplitude volumes within the larger survey for the field of study showing the encapsulated wells

The 3ROIs delineated are named horizon cubes and marked A, B and C (Figure 3). Horizon cube A is 2.6km^2, has 2 wells (m531 and m43), has 88 inlines and 47 crosslines. The offset of the well is 1926m and has proven from earlier interpretation within the zone to be well saturated with hydrocarbon. For horizon cube B, the area is 6.3km^2, has 4 wells (x109, m34, m47, m36). It has 115 inlines and 87 crosslines. Offset distances are as follows; 2000m between wells x109 and m34, 3200m between wells m34 and m47, 1513m between wells m47and m36. Diagonally, 3105 m between wells m36 and m34, 3442 m between wells m47 and x109. Horizon cube C has an area space of 6.5km^2. There are 4 wells within it namely m47, m69, m255 and m52. The cube has 111inlines and 94crosslines. The offset of the wells are 2194m between m47 and m69, 2424m between m69 and m255, 1510m between m255 and m52, 2854m between m52 and m47. Diagonally, there is 2850m between m255 and m47, 3187m between m52 and m69. All zones have appreciable quantity of hydrocarbon and have series of inter-fingerings of sand and shale sequences. Depositional pattern of the field has made mapping of rock units rather challenging laterally prior to the simulation exercise but sequel to that, clearer relationships between rock units and reservoir formations were better defined and fluid properties variation brought to a proper perspective. With the limitations from the seismic attributes library in the Petrel® 2008 software used, one complex attributes was computed (Cosine of Phase), one stratigraphic attribute was computed (Chaos), one structural attribute was computed (Variance), and two waves/velocity attributes were computed (RMS amplitude and second derivative). An attempt was made to additionally compute arithmetically new attributes from the earlier mentioned and the result was new attribute from the multiplication of RMS amplitude with Chaos, and another new attribute from dividing RMS amplitude by Chaos. The following rock properties obtained from various stochastic simulation results were sampled and made into seismic volumes. They are; porosity (Φ), acoustic impedance (AI), permeability (K), hydrocarbon saturation (S_{hc}), elastic impedance 10 (EI10), elastic impedance 20 (EI20), density (RhoB), P-velocity (V_p), S-velocity (V_s), PS-velocity ratio (v_p/v_s) Poisson ratio (σ), and volume of shale (V_{sh}) amongst others that were simulated but not sampled, these few were chosen.

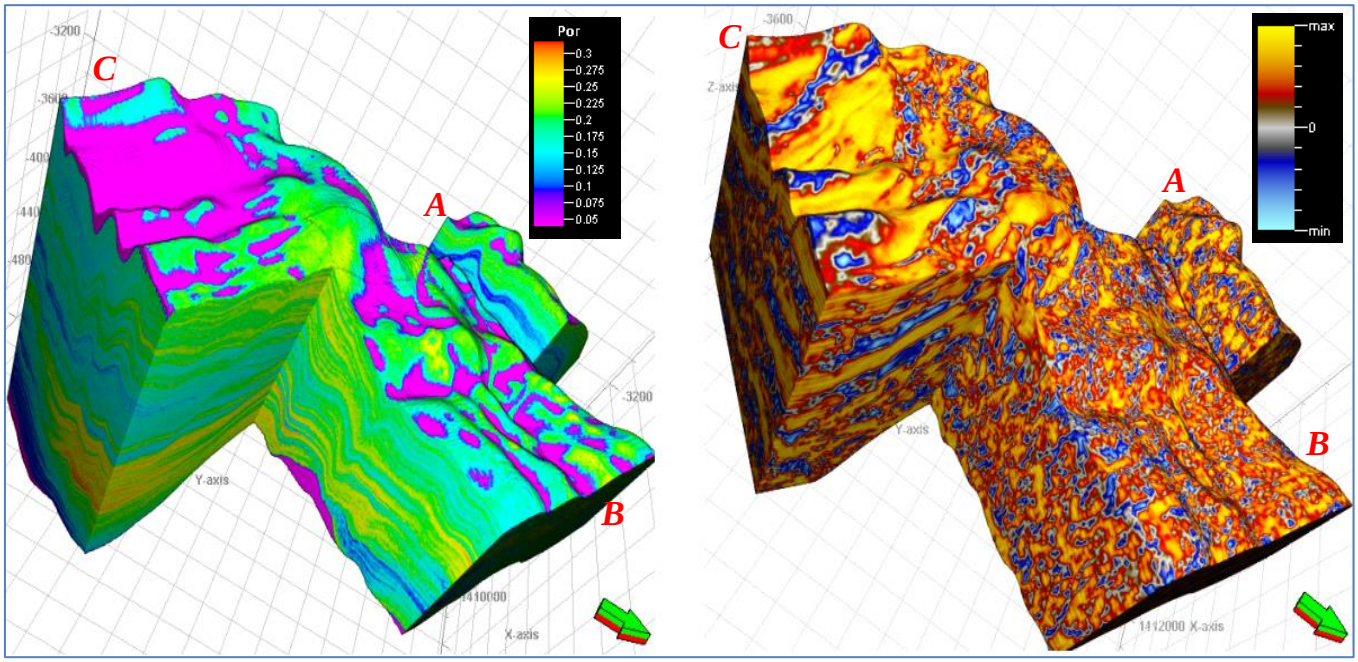

Figure 3 Sculptured horizon cubes of Regions of interest (ROI) for porosity modelled property and RMS amplitude

The approach for defining these relationships is to generate linear functions between rock properties based attributes and also to generate linear functions between seismic attributes. Thirdly, linear function crossplots were also made for relationships between rock properties and seismic attributes. All these three steps were carried out on surface properties captured over different specific depth windows for each horizon cube. Following proper observation their locations were cross-checked with logs and simulations results intersection projections as a control step on the property analyzed. On the surface attributes property capturing, the "about a single horizon" method was chosen as the means of surface attribute extraction. This was due to the dipping and heterogeneous nature of the rock units and accounted for the inconsistencies and fair lateral continuity evident in the turbidites sequences studied. Of all the relationships generated on crossplots, the rock properties attributes appeared to be the best in characterizing the effect of saturation of hydrocarbon (S_{hc}) on the surfaces analyzed. For the rock properties relationships definitions in the function window, S_{hc} was used as the standardizing third variable. This was in view to assist in decision making for hydrocarbon producing level or depth and to highlight the hydrocarbon saturation in the light of other properties of the rock such as porosity, permeability and others (Figures 4 - 9). All the correlation crossplot uses the least square method to define a regression line plot between two visualized variables following which the correlation coefficient, linear function equation and covariance values were obtained.

3. Results and Discussion

3.1 Properties correlations

The rock properties observed in crossplots for horizon cube A has the most reliable correlation coefficient that fall within 0.65 to 0.90 in either negative or positive correlation. Figure 4 shows some of the crossplot for the linear functions between some rock properties. AI against EI20, V_p against V_s, Poisson ratio against V_p/V_s ratio all gave plots with positive correlation coefficient of above 0.8. The other plots of porosity against AI, Rho against permeability, V_p against V_p/V_s ratio, V_p against Poisson ratio, V_{sh} against EI20 and AI against Poisson ratio all had negative correlation coefficients. The color property is hydrocarbon saturation to establish the variation between it and the properties studied. The positions of the wells are strategic in that well x43 locates a more saturated portion in a structural high point (2220 m) accessing the trapping mechanism of the portion while the downward side has the m531 well adequately positioned (2310 m) to drain the distal dipping potion in the southeastern direction. This

location has more of anomalous compaction sediment configuration with no fracture. So the need to recover the heavy hydrocarbon in the presence of competent shale blanket becomes the prevailing challenge. Infill smart wells (for steam injection) locating porous and permeable sand units could be sited at a location between the two wells so as to optimize the draining of the remaining by-passed oil. Or at a point in the life of the producing reservoirs, well x43 could be converted to a steam injection hole since it has been located on a structurally high portion and by gravity flow/ assistance, well m531 can access more of the latent or remaining and by-passed hydrocarbon (Figure 4). In an attempt to characterize the rock units on the basis of the seismic attributes, crossplots were also made of the normal attributes, arithmetically computed attributes and some rock properties. The results show virtually no correlation for all the linear functions generated. Attempted crossplots of RMS amplitude against porosity, variance against porosity, second derivative against porosity, cosine of phase against V_p/V_s ratio, cosine of phase against RMS*chaos all showed no correlation with values around zero (Figure 5). Only the plots of cosine of phase against second derivative came close to 50% correlation coefficient with plots of RMS amplitude against EI20 and chaos against RMS amplitude came with positive and negative approximately 40% correlation respectively (Figure 5). All the second class of plots based on seismic attributes has AI as the third variable to standardize the plot and substantiate the nature of the rock units at each portion on the function plot panel.

Horizon cube B has a different scenario because it has a larger area for analysis and more wells for observation. The rock properties observed in crossplots for horizon cube B just like in A had the most reliable correlation coefficient that fall within 0.75 to 0.90 in either negative or positive correlation. Figure 6 shows some of the crossplot for the linear functions between some rock properties. AI against EI20, V_p against V_s, Poisson ratio against V_p/V_s ratio all gave plots with positive correlation coefficient of above 0.8. The other plots of porosity against AI, Rho against permeability, V_p against V_p/V_s ratio, V_p against Poisson ratio, V_{sh} against EI20 and AI against poisson ratio all had negative correlation coefficients. The color property is hydrocarbon saturation to establish the variation and show the trend between it and the properties studied. Aside the areas space in cube B that is more than that of A, the cube is also faulted as seen in Figures 6 and 7. The positions of the wells are strategic in relation to the faults and structural highs in the area. Wells m34 and m47 were situated on structurally high altitude of 2040m in the southern portion of the distal hanging block of the reverse fault (Figure 6). With this being highly faulted with major faults and more hydrocarbon saturated than other parts, wells were located to access the level where the oil leg is. Well x109 located in the predominantly saturated portion of the cube sits at a structural height of 2070 m while the fourth well m36 occupies a structurally lower location in the western part of the cube though not as saturated as the location of other wells.

This area also has more of anomalous compaction sediment configuration with reverse faults and 3 of the four wells sitting on the hanging wall fault block. The trouble of recovering the heavy hydrocarbon in the presence of competent shale blanket becomes the prevailing challenge more so as the middle portion of the cube is still structurally high due to prevalent rumpling initiated by the compressional force in the formation of the sag structure sequel to the varying strike-slip regime. Hence, optimum drainage of the cube zone will be directed to its western portion and infill smart wells (for steam injection) locating porous and permeable sand units could be sited at a location on the structural high between the four or two wells so as to optimize the draining of the remaining by-passed oil. In this way recovering from the earlier drilled wells (Figure 6). As it was done in the first horizon block, characterizing the rock units on the basis of the seismic attributes resulted in making crossplots of the vintage attributes, arithmetically computed attributes and some rock properties. The results show virtually no correlation for all the linear functions generated. Attempted crossplots of RMS amplitude against porosity, variance against porosity, second derivative against porosity, cosine of phase against V_p/V_s ratio, cosine of phase against RMS*chaos all showed no correlation with values around zero. Only the plots of cosine of phase against second derivative came close to 50% correlation coefficient, with plots of RMS amplitude against EI20 and chaos against RMS amplitude coming close to 25% (Figure 7). Some of these crossplots displayed polarization of variable (i.e. variables plotting on a side or section of the function window). This is seen in the case of the near vertical plot of cosine of phase against V_pV_s ratio, and RMS amplitude against EI20 that appears near vertical and plots of RMS amplitude against porosity, variance

against porosity taking a stand on the far right hand side with positive and negative approximately 30% correlation respectively. All the second class of plots based on seismic attributes has AI as the third variable to standardize the plot and substantiate the nature of the rock units at each portion on the function plot panel (Figure 7).

Horizon cube C is also located in a more distal and dipping portion of the zone. This horizon cube is unfaulted and occurs as a ramp and wedge structure in the distal portion of the larger survey. Rock properties observed in crossplots for horizon cube C had the most reliable correlation coefficient that fall within 0.75 to 0.90 in either negative or positive correlation. Figure 8 shows some of the crossplot for the linear functions between some rock properties. AI against EI20, V_p against V_s, Poisson ratio against V_p/V_s ratio all gave plots with positive correlation coefficient of above 0.8. The other plots of porosity against AI, Rho against permeability, V_p against V_p/V_s ratio, V_p against Poisson ratio, V_{sh} against EI20 and AI against Poisson ratio all had negative correlation coefficients. The color property of hydrocarbon saturation was also used to establish the variation between it and the properties studied. Although no fault was interpreted for this horizon cube well positioning was done predominantly based on the structural highs and within zone stratigraphic traps observed. The positions of the wells are strategic in that well m47 occupies the structurally highest position of 2040 m in the northern part of the zone and at 2194 m away from it well m69 was located at a structurally high depth of 2115 m in the southeastern direction about 75m lower than m47. Well m52 was located on a structural plateau of depth 2190 m and does not seem to locate appreciable amount of hydrocarbon. The southern portion appears as the most hydrocarbon saturated location in the area and it has the portion with the thickest wedge of sediment a distance of 1510 m from well m52. Here well m255 is sited and at the depth 2205 m dipping gently from the ramp initiated from the m52 location (Figure 8).

Heavy hydrocarbon sweeping via steam assisted gravity drainage program will see to it that sequel to initial primary recovery more infill well may be located in the middle portion of this zone to locate the inconsistent stratigraphic traps and also drive the oil to the existing wells for recovery. Secondly, due to the increase of porosity and permeability observed in the sand deposits in this zone, existing wells like m52 could be converted to injection well and if necessary through side tracking deviate the well for the injection fluid to locate the more dipping portions of the zone. However, this distal dipping portion in the southeastern direction is considered most prolific in hydrocarbon saturation because of its more conformable reservoir strata and as it rests against another truncating major fault defining a regional demarcation of strike-slip activities for the study area [14]. The sediment compaction and stratal configuration here is more placid with no faults due to its distal nature from the point of sediment derivation (Figure 8). An attempt was also made to characterize the rock units on the basis of the seismic attributes within this zone, and like the other zones, crossplots were also made of the primary attributes, arithmetically computed attributes and some rock properties. The results for this was not so different from the two earlier discussed. They show virtually no correlation for all the linear functions generated. Crossplots of RMS amplitude against porosity, variance against porosity, second derivative against porosity, cosine of phase against V_p/V_s ratio, cosine of phase against RMS*chaos all showed no correlation with values around zero. Only the plots of cosine of phase against second derivative came close to 50% correlation coefficient. For all this second class of plots based on seismic attributes, AI was used as the third variable to standardize the plot and substantiate the nature of the rock units at each portion on the function plot panel (Figure 9).

4. Conclusions

From the foregoing, it has been proven that more reliable relationships of rock properties as it relates to hydrocarbon occurrence and saturation is obtained and established from direct derivation from petrophysical properties from well logs than that obtained from post-stack seismic data. Therefore the use of well logs derived properties is advocated for better understanding of the nature and characteristics of subsurface rocks in view of hydrocarbon saturation. Although well data comes in bits that does not cover much lateral extent, they are to be judiciously preserved and meticulously handled (when there is limited access to core data) to maximize its benefits as it relates to its use for hydrocarbon exploration.

Acknowledgements

The China Ministry of Science and Technology is appreciated for the equipment donation made available for this research under the CASTEP scheme. TWAS-CAS and Covenant University is also appreciated for the research support.

References

[1] Kearey, P., Brooks, M., Hill, I., 2004, An Introduction to Geophysical Exploration. Blackwell Publishing, 350 Main Street, Malden, MA 02148-5020, USA. Third edition 2002 reprinted 2004. pp. 81-82.

[2] Tsvankin, I, Gaiser, J., Grechka, V., Mirko, van der Baan, and Thomsen, L., 2010, Seismic anisotropy in exploration and reservoir characterization: An overview. *Geophysics*, 75(5) 75A15–75A29

[3] Sheriff, R. E., 1973, Encyclopedic Dictionary of Exploration Geophysics, *Society of Exploration Geophysicists*, Tulsa, OK, pp. 69.

[4] Taner, M. T., Schuelke, J. S., Doherty, R. O', and Baysal, E., 1994, Seismic attributes revisited: 64th Annual International Meeting, *SEG*, Expanded Abstracts, 1104–1106

[5] Brown, A. R., 1996, Seismic attributes and their classification: *The Leading Edge,* 15, 1090.

[6] Brown, A. R., 2004, Interpretation of three-dimensional seismic data, 6th ed.: *American Association of Petroleum Geologists Memoir 42*.

[7] Chopra, S., and Marfurt, K., 2005, Seismic attributes — A historical perspective, *Geophysics,* 70(5), 3–28

[8] Sheriff, R. E., 1992, Basic Petrophysics and Geophysics. In Reservoir Geophysics, R. E. Sheriff, ed., Investigations in Geophysics. 7, *Society of Exploration Geophysicists*, Tulsa, OK, pp. 37-49.

[9] Hilterman, F. J., 2001, Seismic Amplitude Interpretation. 2001 Distinguished Instructor Short Course Series No. 4, sponsored by the *Society of Exploration Geophysicists*, *EAGE*, pp. 2-24

[10] Gassmann, F., 1951, Elastic waves through a packing of spheres, *Geophysics*, 16, pp. 673-685.

[11] Biot, M. A., 1956, Theory of propagation of elastic waves in a fluid-saturated porous solid, *Journal of Acoustic. Society of America,* 28, 168-191.

[12] Barnes, A. E., 2001, Seismic attributes in your facies, *CSEG Recorder.* 9, 41-47

[13] Chambers, R. L. and Yarus, J. M. (2002): Quantitative use of seismic attributes for reservoir characterization. *CSEG Recorder,* 6, 15 – 25

[14] Allen, M.B., Macdonald, D.I.M., Xun, Z., Vincent, S.J., and Brouet-Menzies, C., 1997, Early Cenozoic two-phase thermal subsidence and inversion of the Bohai Basin, Northern China. *Marine and Petroleum Geology,* Elsevier, 14(78), 951-972

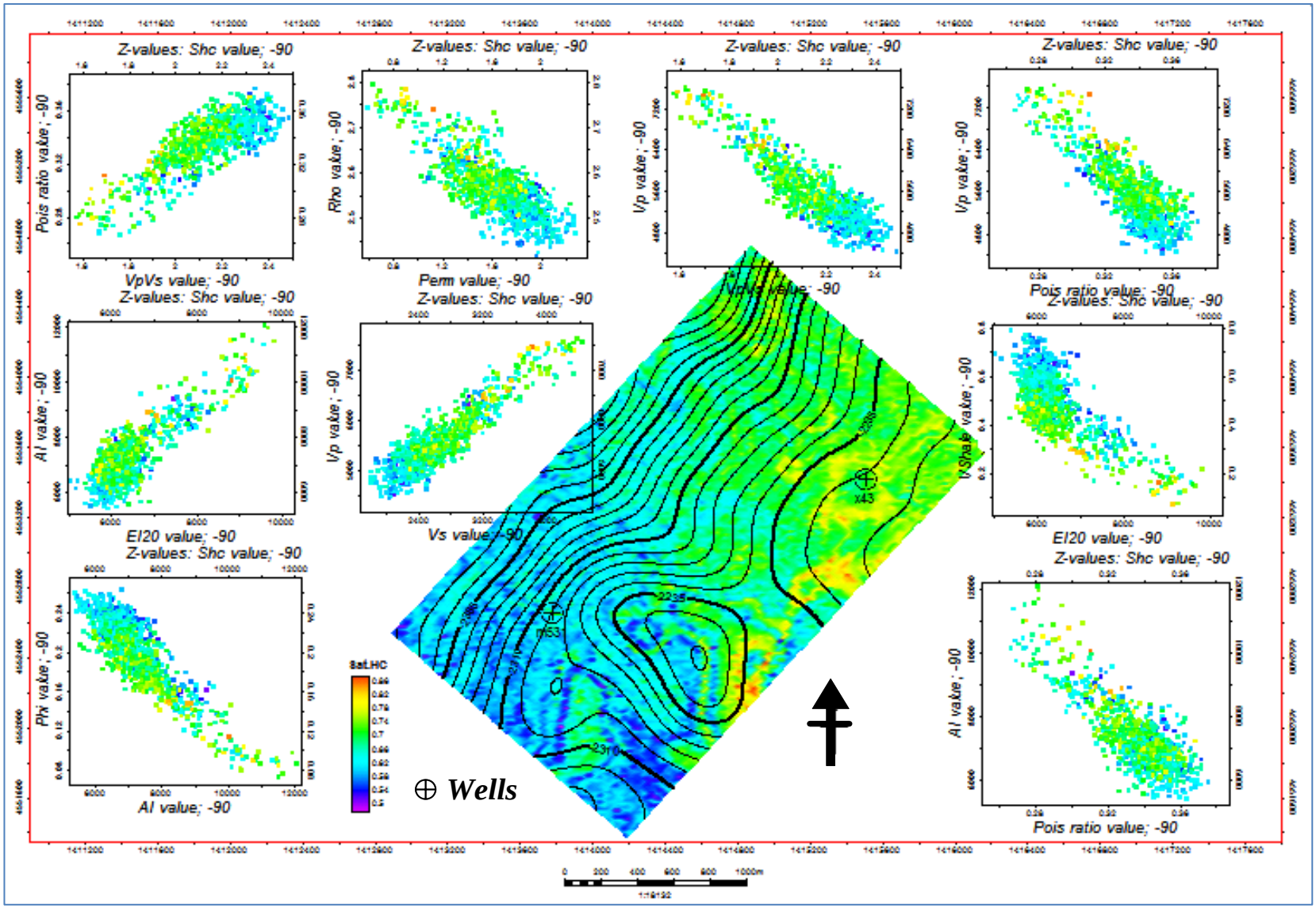

Figure 4 Rock property surface attribute extraction for horizon cube A at 90 m below surface

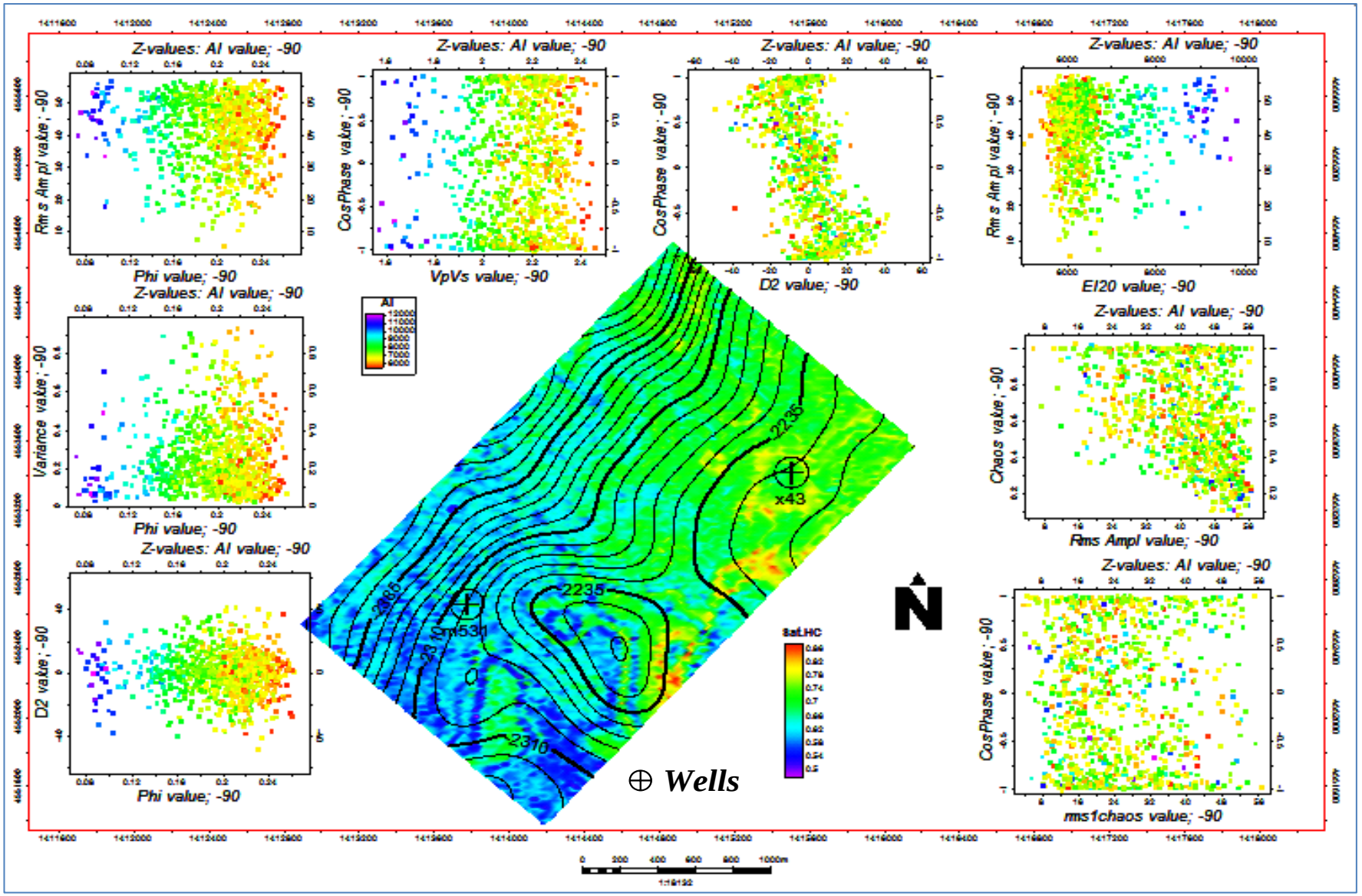

Figure 5 Rock property surface attribute extraction for horizon cube A at 90 m below surface

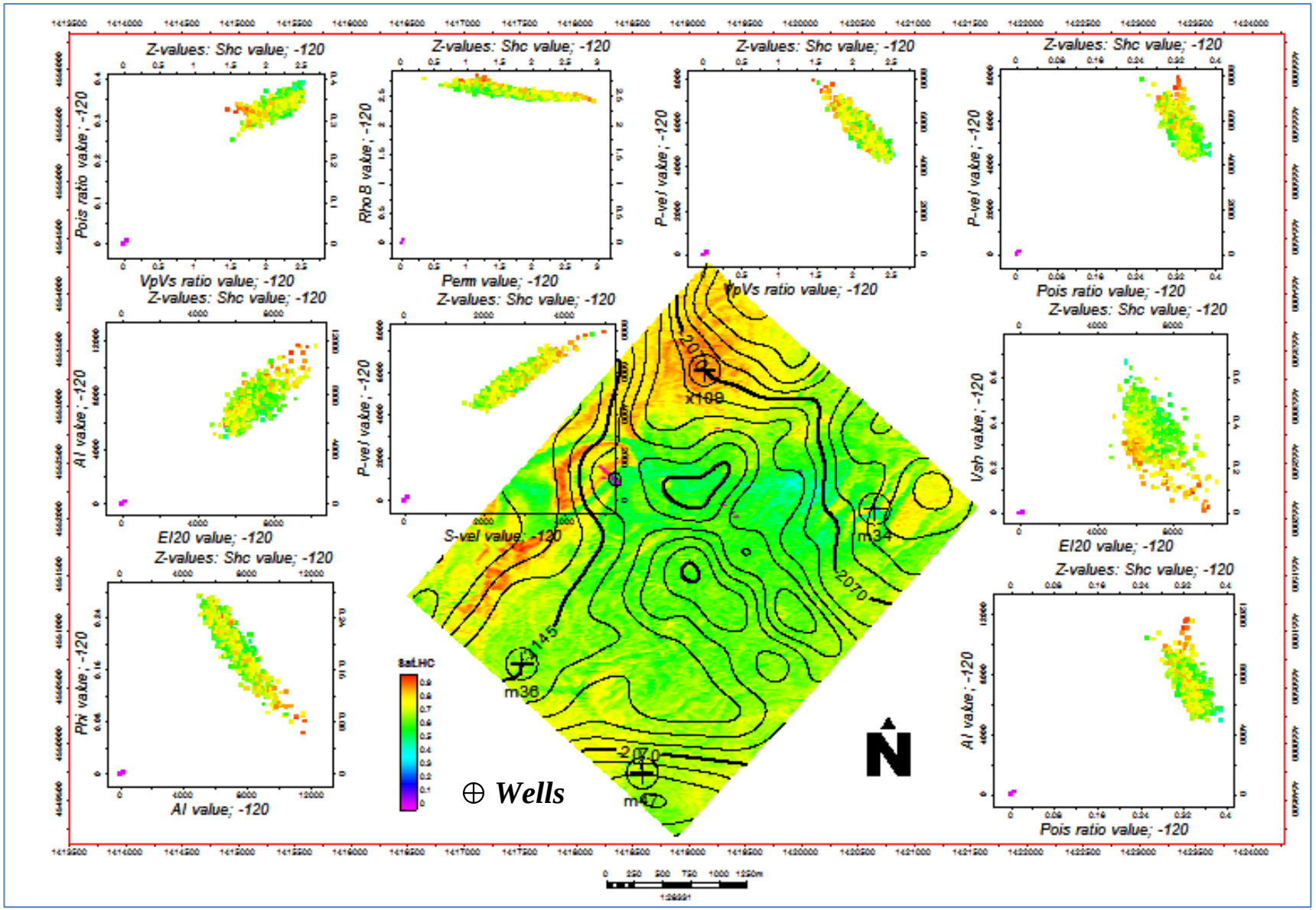

Figure 6 Rock property surface attribute extraction for horizon cube B at 120 m below surface

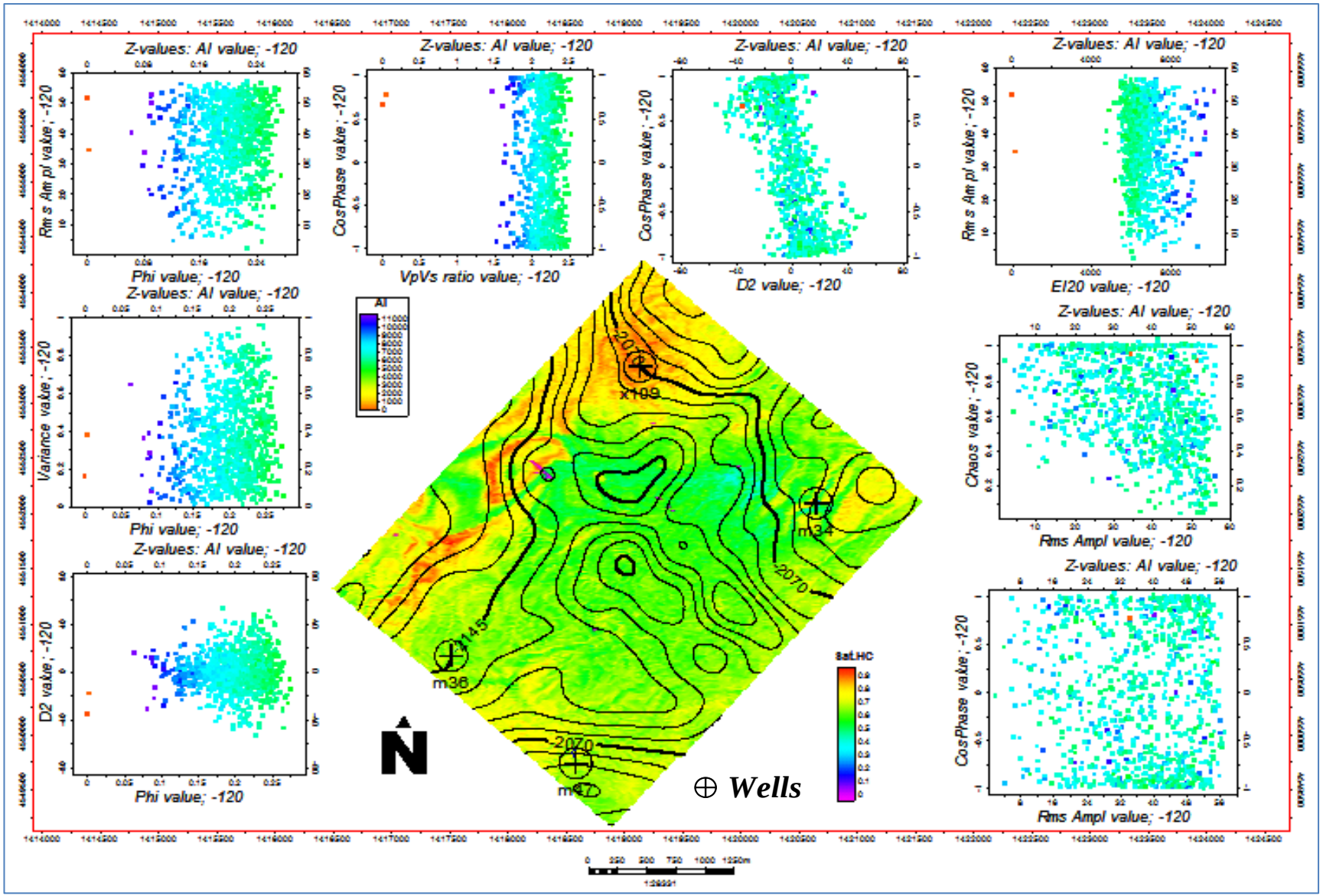

Figure 7 Rock property surface attribute extraction for horizon cube B at 120 m below surface

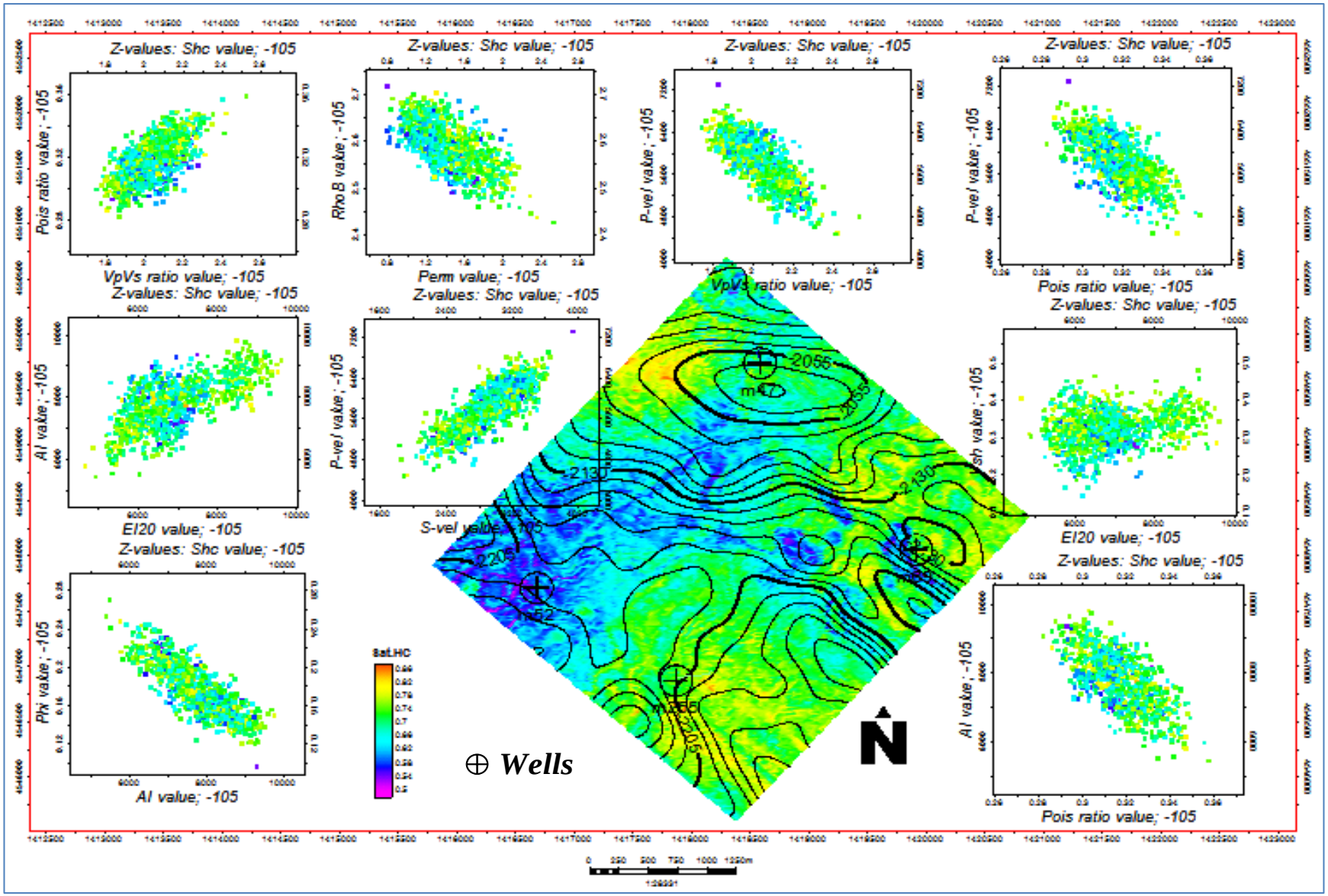

Figure 8 Rock property surface attribute extraction for horizon cube C at 105 m below surface

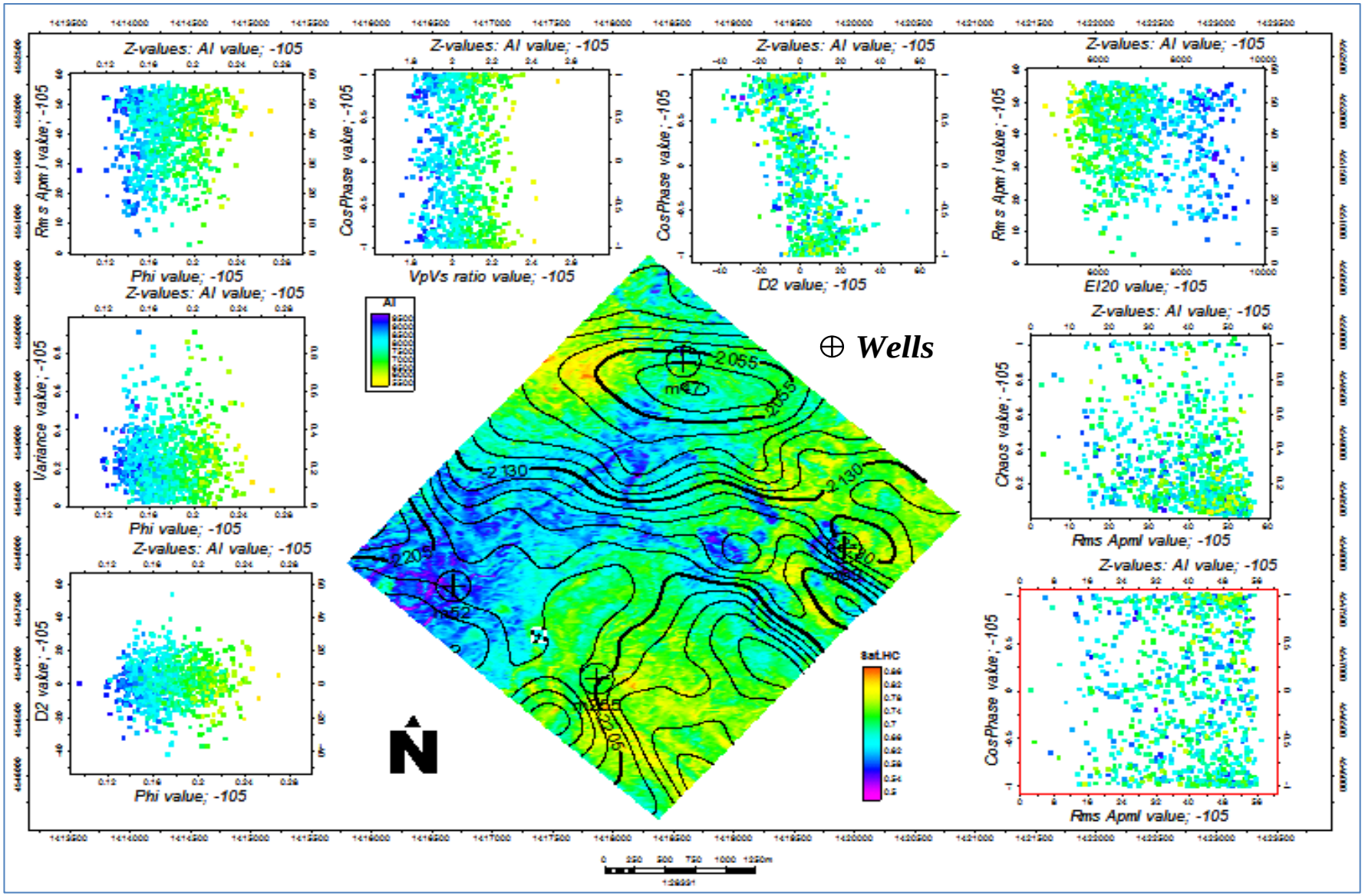

Figure 9 Rock property surface attribute extraction for horizon cube C at 105 m below surface